Section A-Research paper
ISSN 2063-5346

THERMAL MANAGEMENT APPROACH TOWARDS BATTERY OF ELECTRIC VEHICLE

JAVEED AHMAD LONE , M.TECH STUDENT AT RAYAT BAHRA UNIVERSITY PUNJAB , INDIA
EMAIL :lone.javeed199@gmail.com

VARINDER SINGH , ASST.PROFESSOR DEPT. OF MECHANICAL ENGINEERING AT RAYAT BAHRA UNIVERSITY PUNJAB , INDIA
doi: 10.48047/ecb/2023.12.si6.86

A B S T R A C T
Controlling the temperature of a battery pack within an optimal range and ensuring uniform temperature dis- tribution are the key to improving battery life. With the elevating energy density of batteries, more efficient and energy-saving thermal management system is urgently required for improving electric vehicle (EV) performance in terms of safety and long-term durability. In this work, a novel hybrid thermal management system towards a high-voltage battery pack for EVs is developed. Both passive and active components are integrated into the cooling plate to provide a synergistic function. A 35kWh battery pack incorporated with electrical, mechanical and thermal management components was designed, manufactured and integrated. As the core hardware, a pack-level cooling plate set was innovatively designed by integrating with phase change material (PCM). The results show that the combined passive and active cooling strategy ensured a desirable working temperature below 40˚C and a uniform heat distribution across the entire pack at discharging rates ranging from 0.5C to 1.5C under customised control strategies. Moreover, the cycling performance of air cooling and hybrid cooling, as well as the thermal insulation performance at both battery module level and pack level are compared, demonstrating the superior thermal management capability of the hybrid solution.

Keywords:Thermal management Battery pack , Cooling plate , Phase change material Electric vehicle

Introduction

Electric vehicles (EVs) have experienced an explosively high growth with an accelerated market penetration over the past few years [1]. The boom of technology innovation in battery industry, as well as environ- mental, economic and policy concerns around the globe, are firmly presaging a promising prospect of electromobility [2]. Battery pack, the power source of EV consisting of lithium ion batteries (LiBs), has been greatly improved in energy and power densities, round-trip efficiency and operation safety in recent years. However, major

concerns relate to range anxiety, battery longevity and safety are still impeding large-scale EV deployment [3,4]. In parallel to the development of advanced battery technologies, efforts should also be given to improving current battery chemistry, pack design and sub-system performances [5].High voltage battery pack for automotive applications consists of
battery cells, electrical interconnects, controlling units and mechanical structures. It is widely recognized that the electrochemical performance of LiBs is highly dependent on temperature [6]. When the batteries operate at excessively high temperature due to e.g. high charge/ discharge currents, a large amount of heat will be generated and accu- mulated in the limited space within a vehicle. At the cell level, if the heat cannot be dissipated promptly, a continuous rise of cell temperature will induce the damage of solid electrolyte interface (SEI) and the decom- position of the electrolyte, leading ultimately to unwanted safety con- sequences such as thermal runaway. On the other hand, a low temperature operation is not beneficial to the capacity retaining and operation lifespan. In a subzero cold climate, a drastic increase in in- ternal resistance of cell and lithium plating at the surface of anode are main reasons for the capacity to fade. Moreover, resistance inconsistency, unexpected failure of individual cells and inappropriate layout of modules will contribute to temperature maldistribution in the module/ pack. All these issues eventually aggravate to give an unbalanced state of Health (SOH) among cells, which is detrimental to the cyclability of the battery pack. Therefore, it is crucial to secure the battery operation within the desirable temperature range and maintain temperature dif- ference at a low level for maximizing the pack lifespan and usable ca- pacity [6].

In light of improving pack performance, battery thermal manage- ment system (TMS) becomes essential in monitoring and managing the temperature profile. Since the commercialization of passive air-cooled Nissan Leaf [7], TMS has experienced a rapid development in designing and manufacturing to warrant high efficiency and security of EVs. Current TMS utilized in EV industry can be classified into different categories according to active or passive, cooling or warming, air, liquid or using phase change materials (PCMs), or hybridization through combining the above different methods [8,9]. Different TMS technolo- gies have respective characteristics and are applied in various situations. In brief, the selection criteria of a TMS requires comprehensive con- siderations of cooling efficiency, configuration complexity, cost, space constraints and overall performance. Many works have shown efforts in optimization in channel geometry, cell arrangement, etc. for air-cooling. In spite of the low cost and simple devices, the limited cooling capacity of air still restricts its overall performance; comparatively, liquid- cooling provides a more efficient method to achieve better tempera- ture distribution among batteries and can be applied in high heat gen- eration scenarios [10,11]. Nowadays, with an increased power and energy requirement for EVs, liquid-based cooling has become a preferred TMS in major EV products (Chevrolet Bolt, Tesla Model S,
BMWi3 and i8) due to high cooling efficacy [12]. However, liquid cooling also puts an additional burden on the batteries that power the circulation pump. Moreover, the EV industry has recently called for more attention to battery preheating and warming strategies [13]. In this regard, passive thermal management solutions, such as PCM [14] and heat pipe [15,16], combined with active cooling methods are becoming more and more attractive.

Since first proposed by Al-Hallaj and Selman [17,18], solid–liquid PCM-based passive TMS has attracted research interest in the recent decades due to advantages in cost, easiness of handling, high energy storage density and quasi-isothermal storage process. The effectiveness of the use of PCMs to manage heat in battery modules has been exper- imentally and computationally investigated by numerous researchers [19,20]. Considering the intrinsic limitations of organic PCM, which is a widely studied candidate, efforts have been made in various aspects to enhance the thermal properties [21], from compositing PCM with thermal enhancement elements [22] to engineering auxiliary structures, such as heat exchange fins [23]. The problem is that under extreme conditions, once the heat accumulation exceeds the available latent heat of the PCM, temperature will rise rapidly. A promising solution is to couple PCM with an existing active cooling system to form a hybrid TMS, using the advantages of both to achieve an optimal synergistic effect.

Barsotti et al. [24] proposed a simple cooling plate made of graphite- based PCM composite with an embedded U-shaped copper pipe. They conducted numerical simulations to verify the effectiveness of the hybrid cooling plate for a battery module, and the results showed that the intensity and duration of the liquid pumping were reduced. Bai et al. [25] designed a plate-like cooling module, where water flows on the upper part of the plate and a wax based PCM is contained in the bottom part. The plate set was sandwiched with pouch cells, and then the cooling effect was numerically analyzed by varying the geometric pa- rameters and liquid flow rate, which demonstrated that the PCM/water cooling plate decreased the maximum temperature and improved the temperature uniformity. Kiani et al. [26] investigated a hybrid TMS, where nanofluid is used as the active component and metal foam with paraffin is used as the passive component. The numerical and experi- mental results showed that the use of the nanofluid can postpone the onset of paraffin phase transition and prolong the melting time, and hence decreases the temperature ramping rate. So far, most of the published studies on hybrid TMSs have demonstrated the good perfor- mance of PCM with active cooling. However, all the experimental verification tests have been limited to the cell/module level [27]. There has been little work on high-voltage system.

In our previous work, an innovative hybrid-cooling plate (HCP) concept, which is composed of PCM/graphite composite materials and embedded water channels, was proposed [28]. It takes advantage of both passive and active cooling strategies, as well as provides a heating solution to slow down the temperature drop during cold stop. The per- formance of cooling, thermal insulation and temperature uniformity in various environmental conditions was investigated using computational fluid dynamics (CFD) simulations. Results indicated that the HCP was 36% lighter than an aluminum one and 30% reduction in pump energy consumption can be achieved. Our detailed experimental studies at the module level have shown a good agreement with the simulation results, motivating us to validate the HCP performance on a high voltage pack system. Here, the work on scaling our pack level prototype based on the HCP concept and equipped with additional featured structures is pre- sented. To the best of our knowledge, this is a pioneer demonstration to verify the efficiency of the PCM-based TMS in an entire battery pack. Starting with the general considerations in developing a pack pro-totype, the first part of this paper reveals the concrete works of

designing and assembling the high-voltage system equipped with the side-cooling HCPs. Aside from those electrical and mechanical key components, specific focus is given to the development of the novel hybrid thermal management device. The second part reports the testing results, including power capacity of the pack, cooling performance of the HCP under the specific working conditions of batteries and corresponding control strategies, as well as the thermal insulation performance at batteries' resting state. Supplementally, a comparison between the modules with air cooling and hybrid cooling methods is also made in terms of cyclability and temperature distribution.

- ***Customer development of the prototype***

The battery pack design considerations

Considering the difficulty to introduce innovative technology and extra components to a commercial "off-the-shelf" battery pack, a mock- up one with adequate interfaces and sub-systems is manually assembled for demonstrating the desired thermal management performance of the HCPs. Generally, the order of considerations for battery pack design is as follows: (i) the overall design requirement at vehicle level; (ii) the power/energy requirement of the entire battery pack; (iii) the deter- mination of cell type; (iv) the configuration structure of modules; (v) the design requirement of battery management system (BMS) and TMS. In this work, the desired output energy of the battery pack is set as 35 kWh, and the "floor configuration" is determined as the basic packaging architecture.

Based on the convincing results obtained at the module level [28], the NMC battery module, which was assembled in the standard 12S VDA (Verband der Automobilindustrie) format (ZTH E-power Tech Co., Ltd, China), was adopted as the basic configuration block to build the high voltage system. The specifications of the battery cell are listed in Table S1 in the supplementary materials. Using the as-assembled mod- ules can effectively prevent potential failures arising from cell level operations, such as bolt or busbar welding, thus improves the reliability and modularity. Another consideration lies in the perspective of safety. The module-level auxiliary mechanical structures, such as casing and frame, can enhance structural integrity and insulation security of the prismatic cells in the module. Moreover, each module is coupled with a separate battery management unit (BMU) used for collecting status in- formation via compatible communication cables.

The interaction between the battery pack and the external environ-

ment can be achieved through several interfaces, mainly the electrical, mechanical and thermal interfaces. Once the overall goal is determined, more specific considerations can be made.

- ***Electrical aspect***

Based on the specifications of 12S modules and the required energy, some calculations and estimations are given as below:

12S NMC module is used as the base unit, which owns nominal ca- pacity of 51Ah and nominal voltage of 43.2 V.

Eight modules are connected in series to deliver a 345.6 V nominal voltage.

The required total energy is obtained by paralleling two rows of eight modules and configuring an 8S2P structure with a total of 16 mod- ules, capable to deliver 35.2 kWh at the nominal rating.

The battery pack interacts with other EV units (DC/DC, motor controller) to output power and receive live feedback through battery junction box (BJB), in which BMS, fuses, relays, pre-charge resistor are necessarily required for safety (Figure S1 in the supplementary materials).

- ***Mechanical aspect***

In order to determine the type and quantity of the mechanical parts required for the pack construction, the overall volume, available space, internal layout of the pack should be defined in advance. Having the similarity in energy, the commercialized battery system of BMW i3 (Table 1) is chosen as the reference to estimate the basic geometry of our pack.

It can be seen from Table 1 that the BMW i3 (2017 version) battery pack has comparable energy and capacity to our expectations. There- fore, our battery pack is designed with reference to the size and weight of the BMW i3 battery pack, and then it is used to test the performance of the proposed PCM-based hybrid thermal management system.

As shown in Fig. 1, the simplest configuration of the slab-form pack is to arrange the 16 modules in a 4 4 matrix in which two longitudinal rows are electrically connected in series. Additionally, a certain amount of extra space must be considered in order to accommodate the electrical accessories (BMUs, power lines, interconnections with the voltage and temperature couplers), the mechanical supporters (base plate, housing frame) and the thermal management components (HCP, water conduit). It should be noted that the BJB and the coolant circulating system are not included when estimating the pack dimension. They are placed aside the pack and connected with the pack via power lines or water pipes to perform their functions (Fig. 1).

- ***Thermal aspect***

The HCP comprises three parallel water conduits and two cham- bers formed between neighbouring conduits. PCM is then filled into the chambers. As has been investigated at module level, the integrated side- cooling design could ensure sufficient heat exchange among batteries, coolant and PCM, also prevent the potential leakage arising from the material expansion and shrinkage occurred during phase change. To scale up the design and adapt it to pack level, interspace among modules in the longitudinal direction is introduced to accommodate the cooling plates. The length of the cooling plate is extended at least 4 folds while the other geometric parameters are remained the same as per the optimal design at module level. Except for the two outmost cooling plates, three more are shared by the central 8 modules. In total, five parallel cooling plates are connected and converge to the main water pipes at both ends (Fig. 1). In addition to the side cooling strategy, an additional aluminum base plate is located at the bottom of the pack, Specifications of BMW i3 battery pack system (2017).under the modules, which can provide mechanical support and extra cooling capability.

Based on the electrical, mechanical and thermal considerations, the dimensions of the pack system can be estimated in comparison with BMW i3 pack system, as shown in Table 2.

Design and manufacturing of the cooling plate set At the pack level, in addition to length extension, three more features are introduced to the cooling plate set. Firstly, two cuboid structures with orifices are fixed on both ends, through one of which the melted PCM is injected into the chamber while the other servers as an air vent to facilitate filling the PCM. Secondly, in parallel to the conduits, two ribs with the thickness of 1 mm penetrate through the respective chamber, mainly for balancing the in-line pressure and stabilizing such a long plate. The schematic drawing and geometric parameters of a single cooling plate are shown in Fig. 2a and Table 3, respectively. Thirdly, the water conduits, water pipes and main inlet/outlet form fractal archi- tecture, in which the water pipes of five cooling plates converge to the latitudinal channels at both ends by connectors (Fig. 2b). The CAD drawing is detailed in the supplementary materials Figure S2.

- To ensure even flow rates in all the five cooling plates, the flow dynamics was investigated numerically by manipulating the connector diameters, and the optimum values are defined as shown in Table 4. It can be seen that the relative velocity difference among five cooling plates can be well controlled within 2% when 2.5 L/min inlet flow is applied to the main pipe.
- Pack level cooling plates were manufactured using the cold drawing technology. In this way, the variation of the surface roughness of the cooling plate is kept at a low level (<0.5 mm). Before assembling, two key steps were implemented to complete the HCP preparation. Firstly, the as-prepared PCM (preparation procedure and thermal physical properties described in the supplemental materials) should be filled into the chambers of cooling plates, and the procedure is described as fol- lows: PCM was heated up to above 35°C in an oven with the assistance of sufficient agitation; then the melted PCM was filled into the chambers of the cooling plates. To ease the impregnation procedure, the cooling plate was placed obliquely and heated by circulating warm water. Secondly, a thin layer of silicone heat conductive paste (KT801, 5 W/m·K, KOVOST, Shenzhen) was scribbled on the contact surface of the cooling plates and the batteries. In this way, heat transfer can be further enhanced by eliminating potential air voids at the interface.

Additional key components

Additional key components refer to the mechanical (cover, frame, bottom plate) and electrical parts (BJB, busbar, cables), comprising the basic structure of the battery pack (Fig. 3). The mechanical components provide protection from vibration and external crush. More importantly, electrical components have power transmission, communication and control functions. The specifications of these key components are sum- marized in Table 5.

It is worth mentioning that, compared with the common bottom cooling design, in the side-cooling design, special attention should be paid to the contact thermal resistance between the HCP and modules. To maximally alleviate negative effect from thermal contact resistance and enhance the integral stability, a "fastener" structure between side frames and exterior

cooling plates was customized to provide an efficient normal constraint. Another crucial consideration lies in the compact design, which is very demanding for improving systematic energy den- sity of the pack. However, for the current prototype, the internal space was not optimally utilized, as shown in the blue marked part in Fig. 3.

Table 1

Item	Size/mm × mm × mm	Volume /L	Weight/ kg	Nominal voltage/V	Total capacity/ Ah	Total energy/k Wh	Cooling system
Value	160×964 ×174	278.5	256	352	95	33	Refrigerant based

Table 2
Dimensions of the self-developed battery pack.

	L (mm)	W (mm)	H (mm)	V(L)
Module (12S)	355	151.5	107.8	6
16 modules	1420	606	110	95
Pack + cooling plates + base plate	1950	830	173	280
BJB	900	700	201.5	126
BMW i3 battery pack with liquid cooling	**1660**	**964**	**174**	**278.4**

Section A-Research paper
ISSN 2063-5346

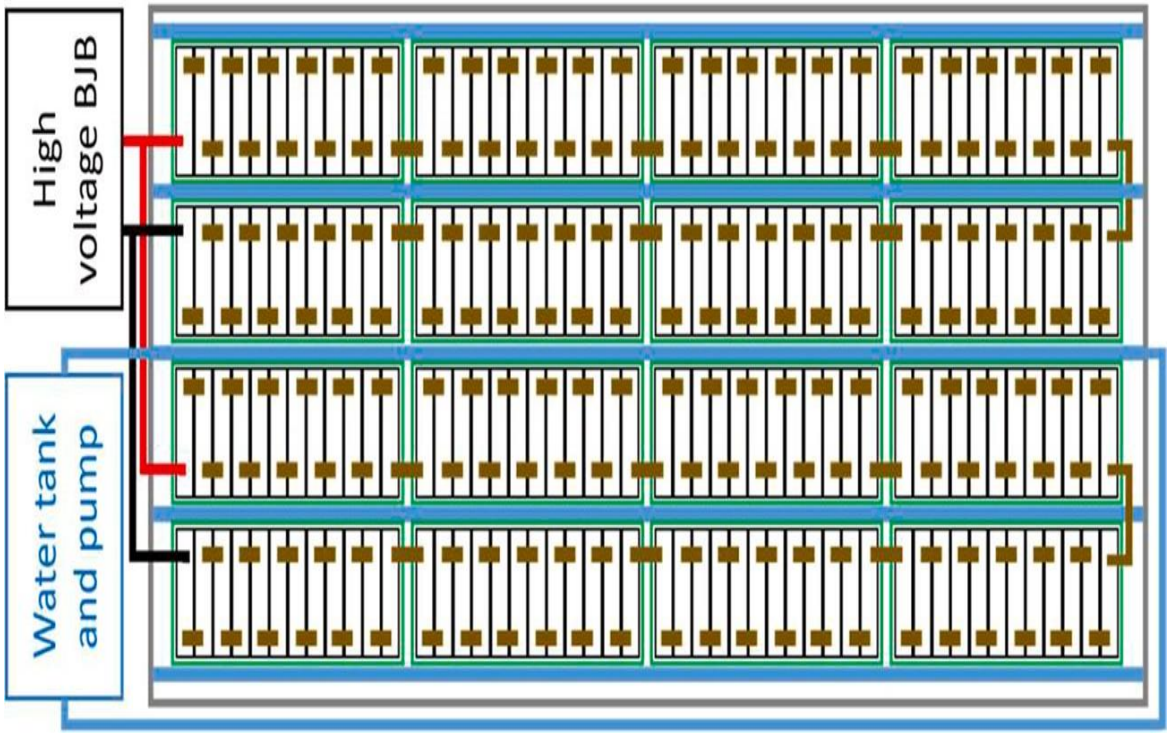

Fig. 1. Schematic diagram of the battery pack.

Table 3
Parameters of single cooling plate.

Length (mm)	Height (mm)	Width (mm)	Wall thickness (mm)	PCM chamber cross section (mm × mm)	Water tube cross section (mm × mm)
1476	87	8	1	33 × 6	4 × 6

The modules and BMUs were assembled according to the structural diagram shown in Fig. 4. By integrating those subsystems and compo- nents, the final battery pack prototype was obtained, as presented in Fig. 5.

Section A-Research paper
ISSN 2063-5346

Table 4

Connector diameters and corresponding inlet flow rates of cooling plates.

Plate number	1	2	3	4	5
Φ (mm)	10	9.1	8.6	9.1	10
$\dot{V}$(L/min)	0.503	0.495	0.504	0.496	0.503

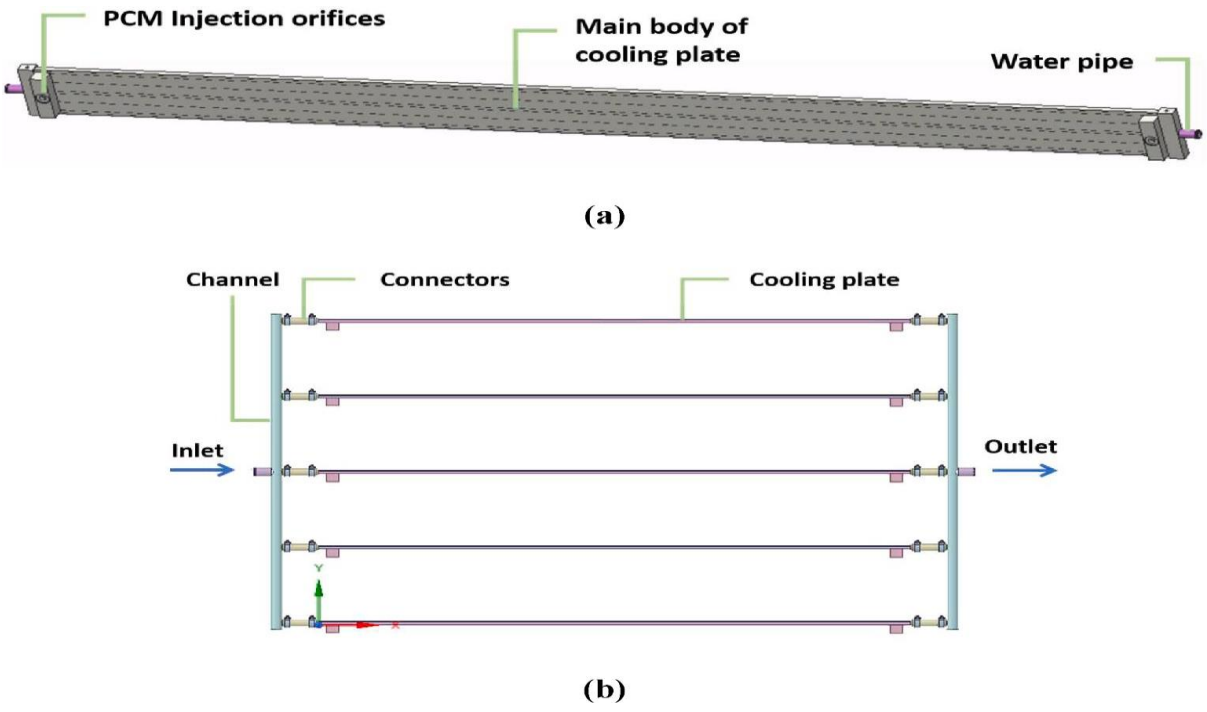

Fig. 2. (a) Scheme of the single cooling plate; (b) Top view of the cooling plate set.

Section A-Research paper
ISSN 2063-5346

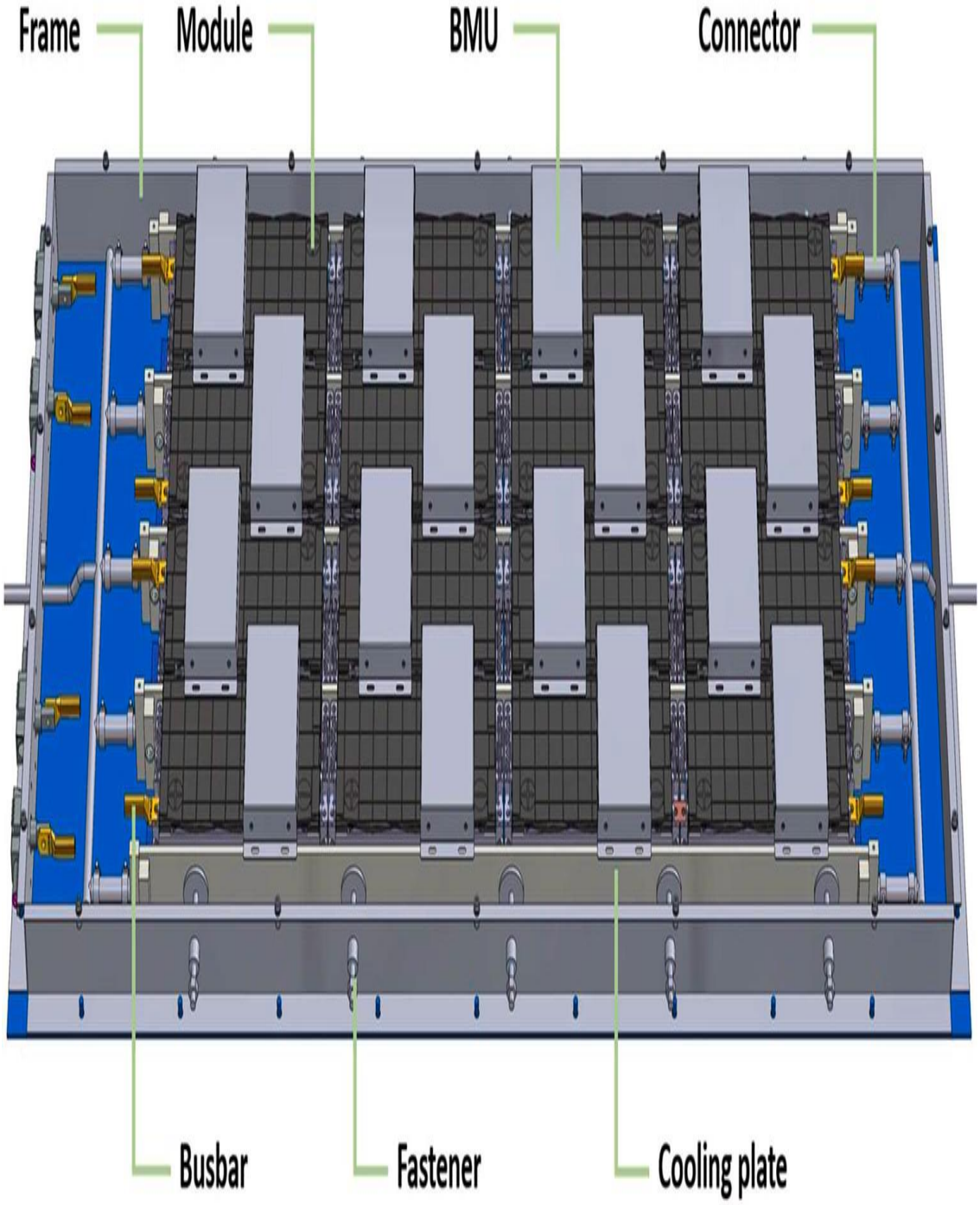

Fig. 3. Breakdown structure of the key components in the pack.

Table 5

Specifications of key components of the battery pack system.

Item	Supplier	/ Material	Weigh	Am	Gross	weight

	manufacturer		t (kg)	ount	(kg)
Base plate	Fengkai Heat	6061Al	17.5	1	17.5
End plate 1	Exchanger Co. Ltd. Beijing	Q235 carbon steel	4.4	2	8.8
End plate 2		Q235 carbon steel	1.65	2	3.3
Mandrel		Q235 carbon steel	0.15	8	1.2
Cover plate		Q235 carbon steel	29.1	1	29.1
Modules	ZTE E-Power Co. Ltd.	–	11.6	16	185.6
Cooling plates	Fengkai Heat Exchanger Co. Ltd. Beijing	6061Al	1.2	5	6
Channels	Fengkai Heat Exchanger Co. Ltd. Beijing	6061Al	1	2	2
Connectors	Fengkai Heat Exchanger Co. Ltd. Beijing	304 Stainless Steel	0.3	10	3
BMU	Pingdan Tech. Co. Ltd.	–	1	16	16
Busbar	Fengkai Heat Exchanger Co. Ltd. Beijing	T2 copper	0.08	16	1.28
Power supplier	Fengkai Heat Exchanger Co. Ltd. Beijing	Φ50 copper wire	1	1	1
Data collector	Tianneng Co. Ltd.	–	3	1	3
Total weight					277.78

presents the detailed mechanical fixing structure. In particular, the bottom plate and side frame are mounted together by screws. Five pairs of fastening pieces (mandrels), composed

Section A-Research paper
ISSN 2063-5346

of threaded rods and wheels, are pressed on the exterior wall of the HCP and exert latitudinal force opposingly to ensure firm contact between the cooling plates and the modules (Fig. 6b). In order to prevent the HCP from deforming under the force of the fastener, a gasket is placed between the HCP and the wheel.

Electrical system

Inside the pack, 16 modules are electrically connected in 8S2P configuration. Each module is equipped with an individual BMU which

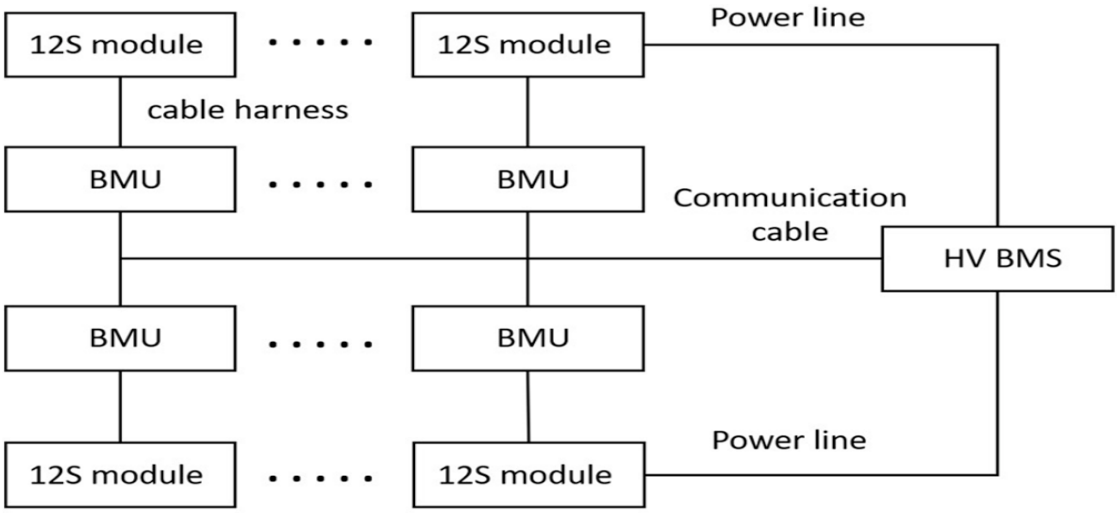

Fig. 4. Schematic diagram of the high-voltage battery pack system.

monitors the voltage and temperature status of the 12 batteries (Fig. 7a). The status information of each single cell is then transmitted to the central BMS in BJB by the cable harness (Fig. 7c). In addition to communication, BJB also provides high-voltage interface with the bat- tery pack via two output power lines (Fig. 7b).

Thermal management system

In Fig. 8, the overall and partial structural features of the HCP are presented. The smooth surface of the HCP maintains good thermal contact between the plate and modules (Fig. 8a). Local view over the HCP terminal is given in Fig. 8b. Within the water splitter, inlet flow distributes to three pathways. A vent plug is installed for adjusting in- ternal pressure when the flow rate alters. After filling PCM and sealing, five HCPs are mounted within the battery pack in a parallel manner, as shown in Fig. 8c. It is also noted that all HCPs converge to the main water channels at both ends via the designed connectors with specific sizes.

Test setup of the developed battery pack

The pack test platform

To perform the pack level tests, a platform including high-voltage tester (Techpow Electric Co., Ltd., ~1000 V, ~400A/channel, 4 chan- nel) and cooling equipment (Beijing SSOSCH Co., Ltd., Deep cooling

series, <40 L/min, <2bar, 40-80˚C) was established according to Fig. 9.
The whole system operates according to the instructions from the PC to the tester (charge/discharge rates) and the cooling system (control strategy). In addition to the passive cooling function, the liquid cooling strategy could be customized according to the specific temperature o

(a)

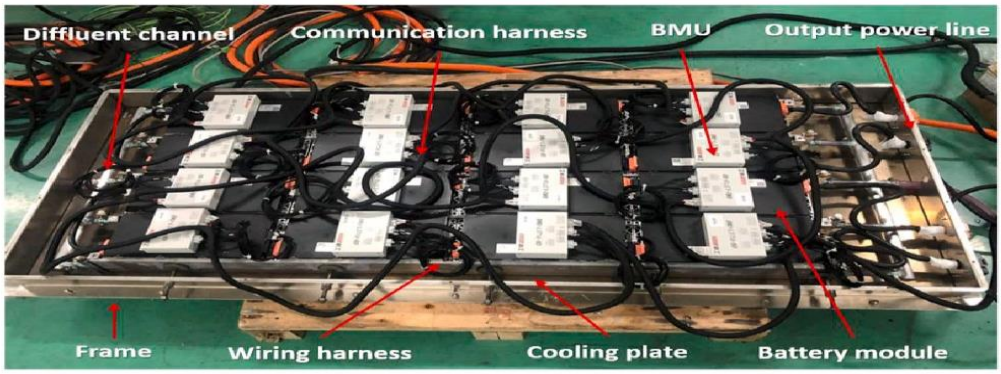

(b)

Fig. 5. (a) Battery pack prototype, and (b) key components inside the pack.

the battery pack when it works under different conditions. For this purpose, 32 thermocouples were utilized to monitor the real time tem- perature evolution for the whole pack. As shown in Fig. 10, considering that the high temperature is commonly detected at the tab regions [29], two thermocouples were placed on the positive and negative terminals of each module.

Control strategy

All the pack level tests were carried out at a constant environmental temperature of 25 ˚C. In order to evaluate the thermal management performance, the pack system was cycled at identical charge profile defined in Table 6, where different discharge rates, 0.5C, 1C and 1.5C, are specified. For simplification, the charging segment is expressed as 1C in the following text. Within each cycle, the pause time between charge and discharge was adjusted according to different discharge conditions and active cooling strategies.
The general aim of designing the control strategy is to assure the pack working at the optimal temperature range of 15-35˚C and maintain uniform temperature distribution assessed by the maximum tempera- ture difference, ΔT, defined by Tmax-Tmin. Accordingly, the upper and lower critical temperatures, TH and TL, at which the active cooling starts or stops, as well as

the inlet water temperature, Tw, and flow rate, V˙, are modified under different working conditions. Fig. 11 indicates the general control strategy. Considering the hysteresis of temperature decrease after activating the water cooling, the critical value of ΔT is set to 6 ˚C and 8 ˚C respectively in the passive-only and hybrid cooling sections.

Through trial and error, the thresholds, TH and TL, for all case studies were set to 31˚C and 24˚C, respectively. Then, main effort was made to adjust the liquid flow rate V˙ and the inlet water temperature Tw. The final optimal parameters in the control strategy are given in Table 7.

Results and discussion

Power capacity

The battery pack capacity and the stored energy during the initial five cycles at 1C discharge rate is shown in Fig. 12. The test results show that the actual battery pack capacity and energy are in line with ex-

pectations, which present 101.97Ah of capacity (Ucrel = 0.152%) and

35kWh of energy (Ucrel 0.180%) for the 8S2P electrical configuration. The uncertainty analysis for the obtained capacity, energy and tem- perature is provided in the supplementary materials in detail.

Cooling performance

According to the customized control strategy described in Section 3.2, the maximum temperature of the pack, Tmax, can be well controlled below 35˚C and the maximum temperature difference, ΔT, can be maintained within 8˚C through the synergistic effect of PCM and water cooling. In the case of 1C discharge rate as shown in Fig. 13, the highest Tmax and ΔT appear at the end of 1C charge segment. Besides, the evo- lution of Tmax and Tmin (Fig. 13b) indicates two operation periods of active cooling, one is from the middle of 1C charge to the end of 0.2C charge, the other is from the middle of 1C discharge to the middle of the following pause. In other words, the working time of the water cooling system accounts for approximately 40.7% of a complete cycle. During the remaining 59.3% of the cycle, only the PCM plays the cooling role, and ΔT is always maintained at a relatively low value between 2 and 3˚C, which means that the passive management components can effectively absorb heat. Furthermore, from the beginning of water cooling to the end of discharging, an obvious plateau with Tminat 28˚C was detected, as shown in Fig. 13 (b). This phenomenon indicates the occurrence of the phase change process of the PCM. However, because the discharge time is not long enough and no more heat is generated, it is difficult to know whether the PCM is completely phase changed in this test.

The control strategy for 1C/0.5C cycling has been modified based on

the general one given in Section 3.2. After several cycles, it was found

Section A-Research paper
ISSN 2063-5346

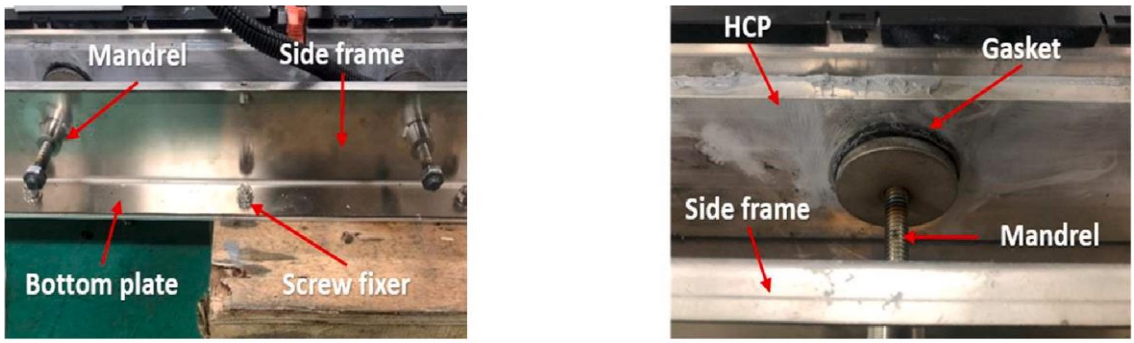

(a) **(b)**

Fig. 6. (a) The mechanical fixing design, and (b) structure of the fastening pieces.

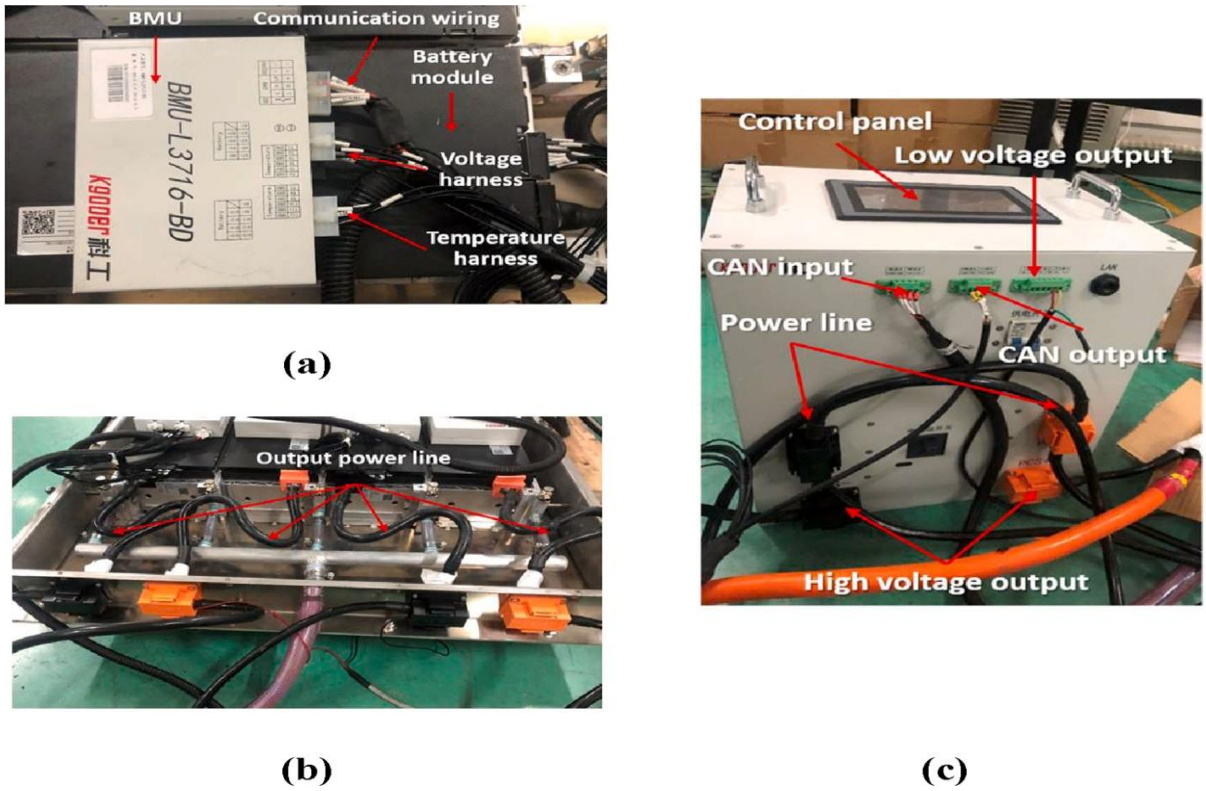

(a)

(b) **(c)**

Fig. 7. (a) BMU, (b) output power line, and (c) connection with BJB.

Section A-Research paper
ISSN 2063-5346

(a)

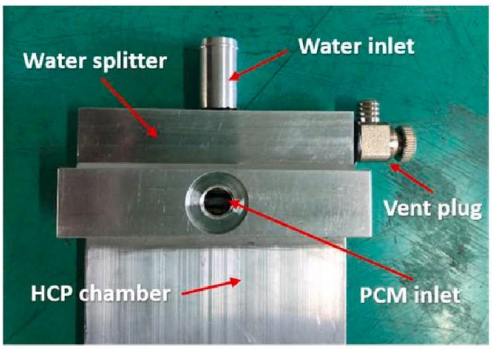

(b)

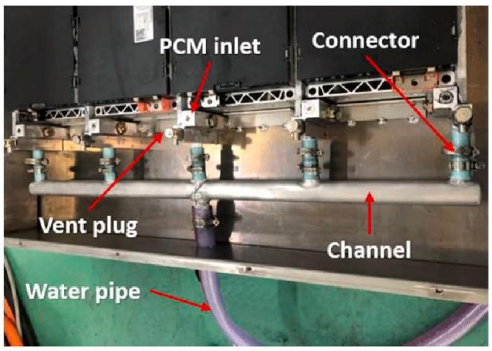

(c)

Fig. 8. (a) HCP overview, (b) terminal structure of the HCP, and (c) HCPs with specific connectors in the pack.

that passive cooling capacity was adequate to sustain the 0.5C discharge segment. Till the end of discharging,Tmax stayed below TH and ΔT retained well around 4˚C, thus the active cooling was not triggered. However, natural convection was insufficient to promote rapid heat dissipation to the air, partially due to the thermal insulation effect from PCM. This may aggravate drastic rise of temperature in the following charge segment. Therefore, the active cooling was enforced during the 1 h pause between discharge and charge. In the end, the overall ΔT in 4 cycles was controlled stably below 6˚C and the active cooling working time contributed approx. 34.4% to a full cycle (Fig. 14).

Noticeably, a temperature plateau is observed during discharge segment. It is believed that during the 40 min, the heat generated from cells is mainly absorbed by the PCM until the saturation of latent heat. Based on this assumption, the average heat generation can be estimated easily based on the known PCM specifications:

Section A-Research paper
ISSN 2063-5346

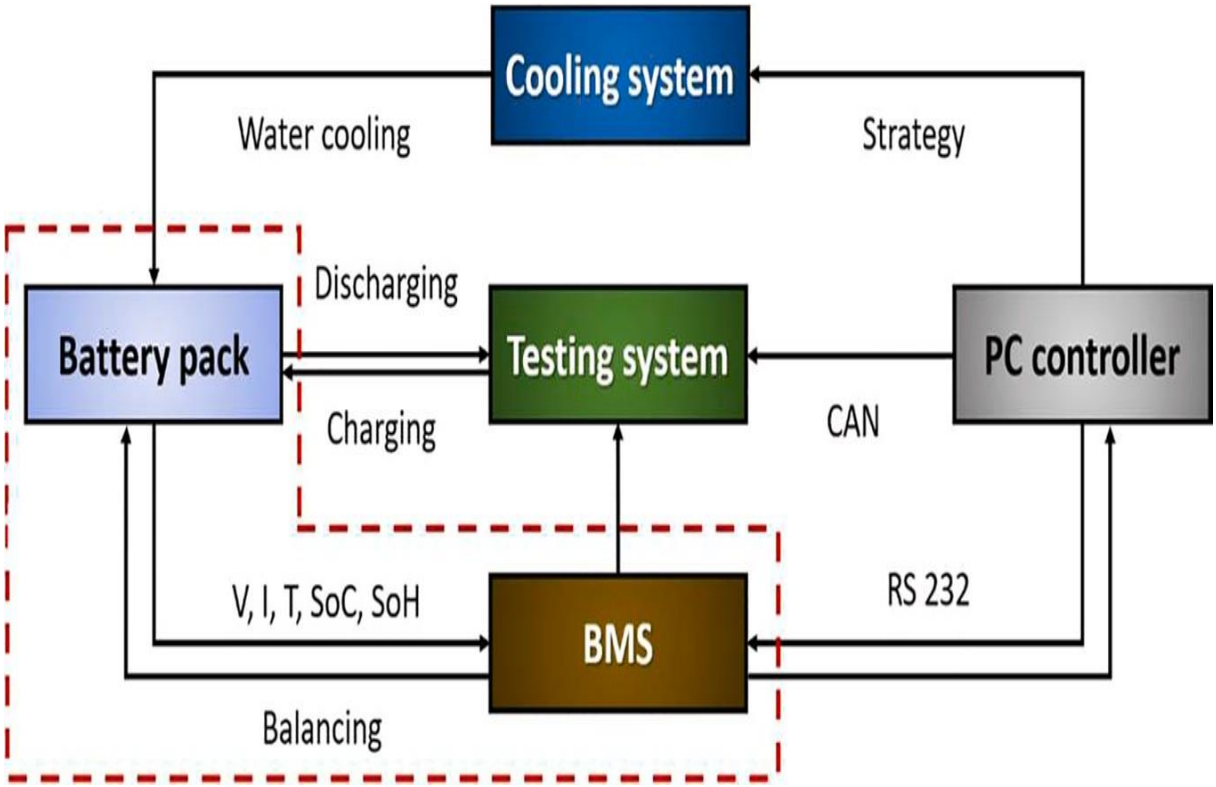

Fig. 9. Hardware connection diagram.

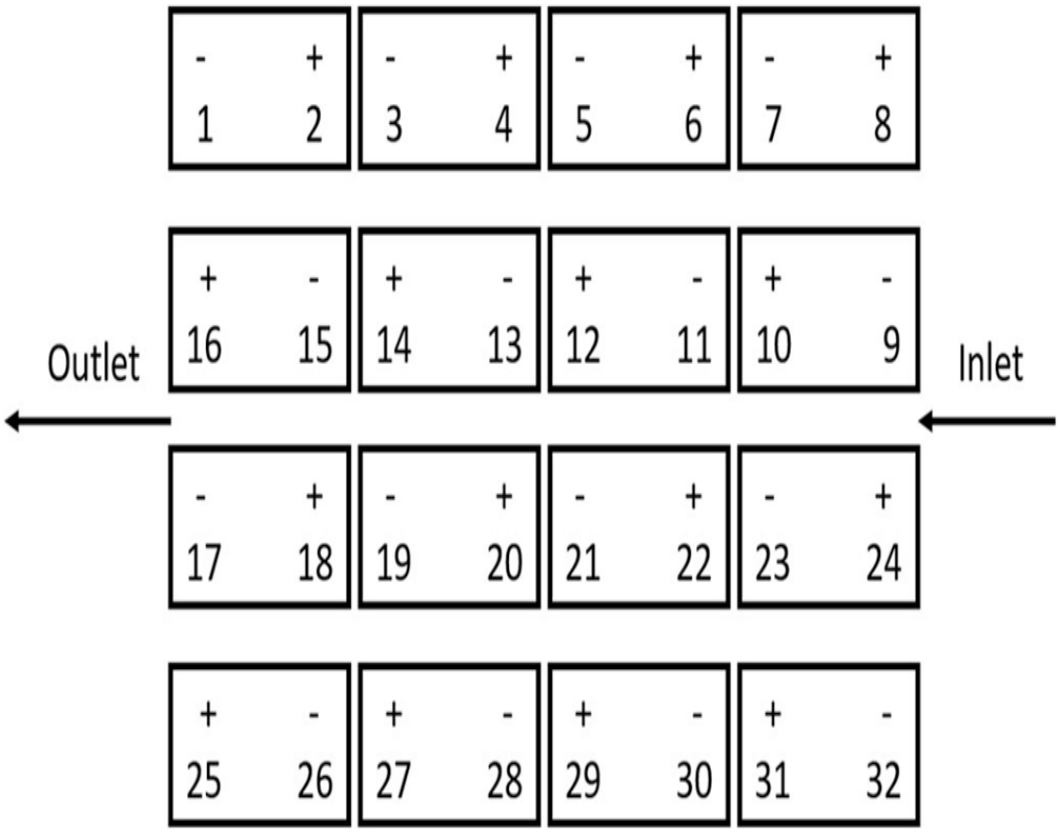

Fig. 10. The locations and numbers of the thermocouples.

Table 6

Section A-Research paper
ISSN 2063-5346

Battery pack charging profile.

Battery pack charging profile.

Charging profile Step	Action	C-rate	Limit
1	Charge	1C (102A)	$U_{cell\_max} \geq 4.2$ V
2	Pause	–	10 min
3	Charge	0.5C (51A)	$U_{cell\_max} \geq 4.2$ V
4	Pause	–	5 min
5	Charge	0.2C (20.4A)	$U_{cell\_max} \geq 4.2$ V

Table 7

Parameter settings of the cooling strategy.

C-rate	$\dot{V}$(L/min)	T_w (C)	T_H (C)	T_L (C)
0.5C (51A)	14	15	31	24
1.0C (102A)	16	12	31	24
1.5C (153A)	19	10	31	24

Parameter settings of the cooling strategy.

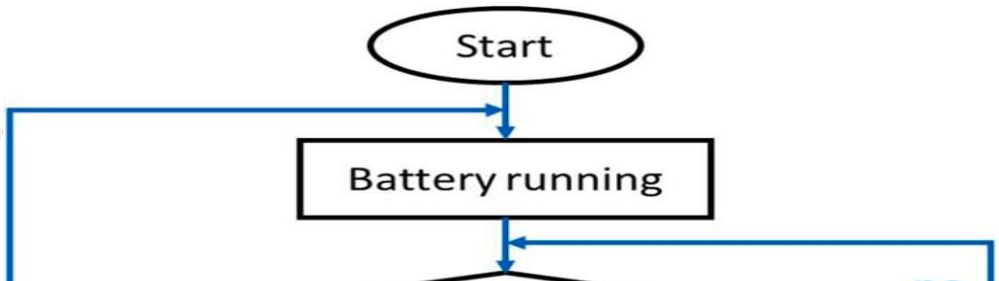

Section A-Research paper
ISSN 2063-5346

fig. 12. Capacity and energy at 1C discharge.

P Lpcm × mpcm
t × 196
(1)

where Pcell is the averaged heat generation power per battery cell; Lpcm is the latent heat of the PCM, 150 kJ/kg; mpcm is the total mass of the filled PCM, t is the plateau duration.
According to Eq. (1), the obtained power is 1.59 W per cell. In addition, the averaged electric resistance rcell can be calculated as follows:
rcell = Pcell
where I is the electric current.
According to Eq. (2), the rcell is 2.4 mΩ, which is reasonable.(2)
Fig. 11. Flow chart of the general control strategy.Under the 1.5C discharge condition, large amount of heat was generated in 40 min. The maximum temperature in the pack was detected to approach 40˚C. Even at full capacity of active cooling (V˙ 19 min/L, Tw 10˚C), it was hardly to constrain Tmax below 35˚C, despite that the combined passive and active cooling significantly moderated the steep temperature ramping during discharge segment, as shown in Fig. 15. In addition, ΔT remained around 7˚C during the full cycle which also approached the as-set limit. Basically, PCM played a subordinate role under harsh conditions, such as high C-rate. In such scenario, it is

Section A-Research paper
ISSN 2063-5346

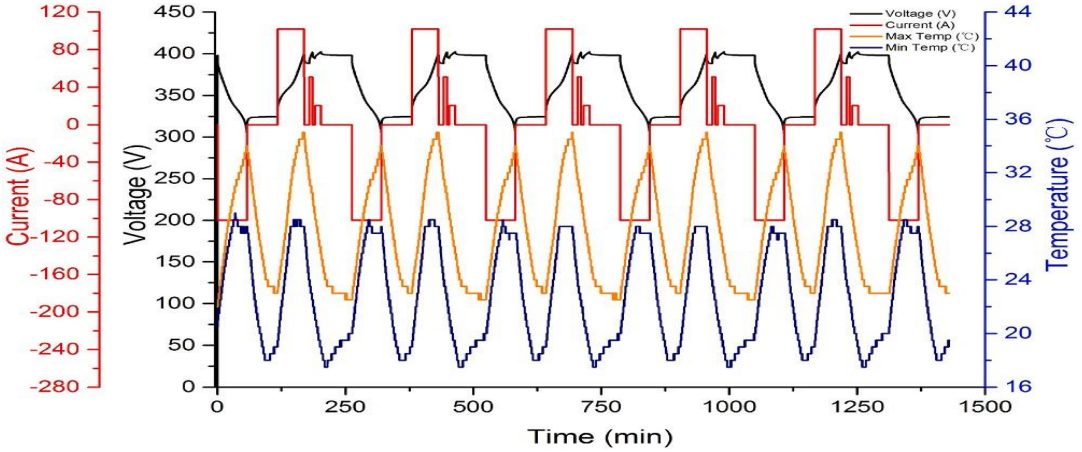

(a)

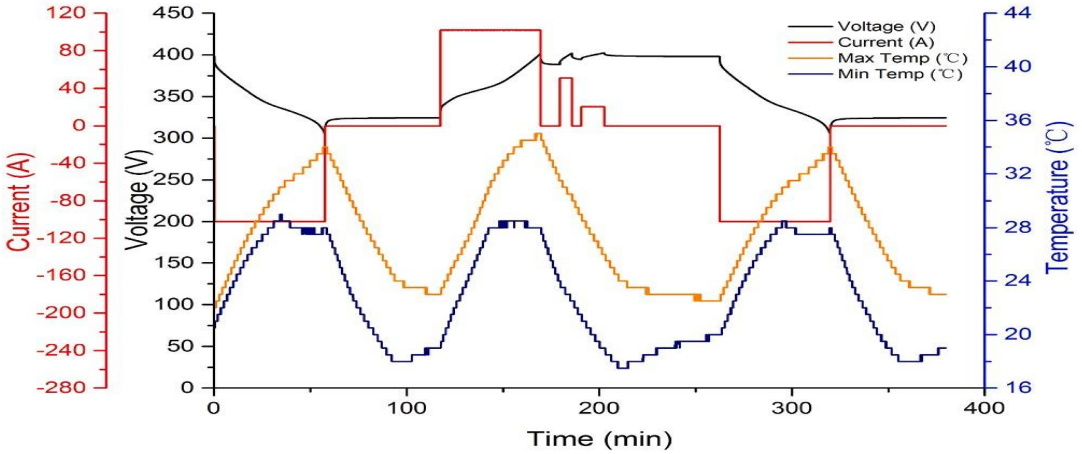

(b)

Section A-Research paper
ISSN 2063-5346

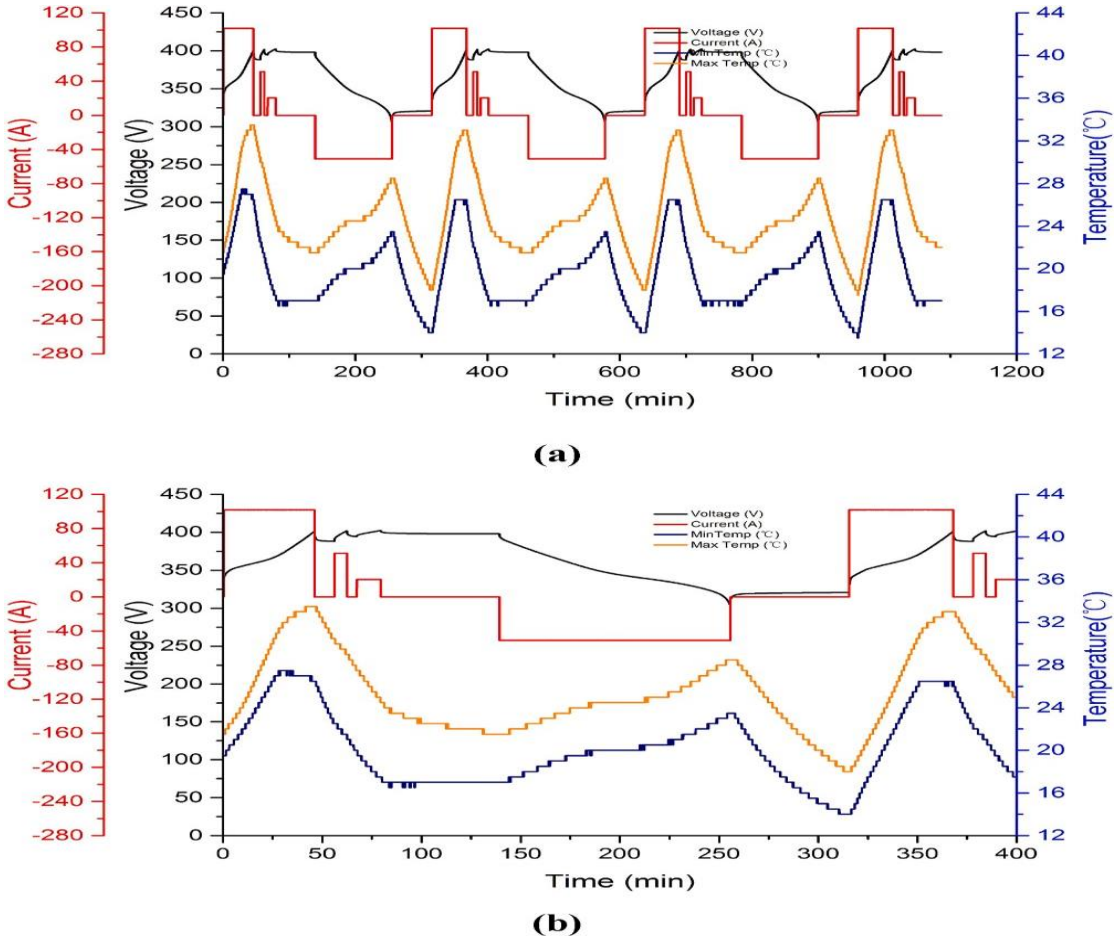

Fig. 13. Cycling performance of the battery pack at 1C discharge rate: (a) 5 cycles, and (b) 1.5 cycles.

suggested to supply the pack with longer time of active cooling, e.g. setting lower TH. The substitute of water with coolant (ethylene glycol solvent) can also be an alternative solution.

Module cycling

In addition to the test at the battery pack level, the effect of the hybrid cooling strategy at the module level was also evaluated. For comparison, two modules were prepared, one of which was equipped with scaled-down HCPs, and the other was equipped with air cooling (AC) channels and fans. The CAD drawings and photos of two modules are provided in the supplemental materials as Figures S3 and S4. In order to compare their thermal management performance, both mod- ules were cycled at 100% depth of discharge and 1C rate, based on the specified cooling strategy shown in Table 8.

Effective thermal management is an important factor in improving battery cycle life. Fig. 16 shows the capacity retention of the two modules up to 50 complete cycles with a continuous degradation ten- dency. The normalized capacity retention of the AC module decreases slightly faster than that of the HCP module, indicating the effectiveness of the hybrid cooling strategy.

In order to monitor the local temperature changes during cycling, 12

thermocouples were deployed on the top surface of the module assem-

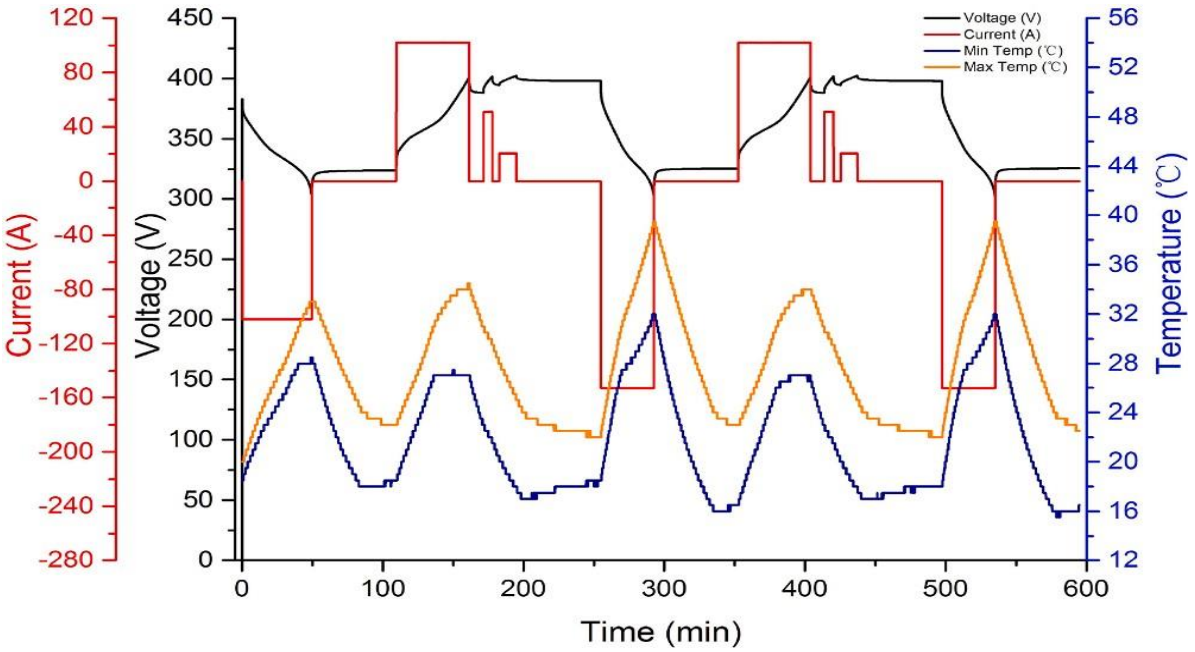

Fig. 14. Cycling performance of the battery pack at 0.5C discharge rate: (a) 3 cycles, and (b) the initial cycle.

Fig. 15. Cycling performance at 1.5C discharge rate.

Table 8
Parameter settings in the battery module test cooling strategy.

Module	Capacity	T_w (C)	T_H (C)	T_L (C)
Hybrid cooling	$\dot{V} = 2$ L/min	25	35	27
Air cooling	$P = 10$ W	On		

each cell. Fig. 17 (a) and (b) show the Tmax and Tmin recordings of the AC module and the HCP module for the initial 3 cycles. Till the end of discharging, Tmax and ΔT of AC module approach 47˚C and 13˚C, respectively. Comparatively, for HCP module, Tmax is well controlled below 35˚C and ΔT is only 5˚C, indicating more efficient heat dissipation

Section A-Research paper
ISSN 2063-5346

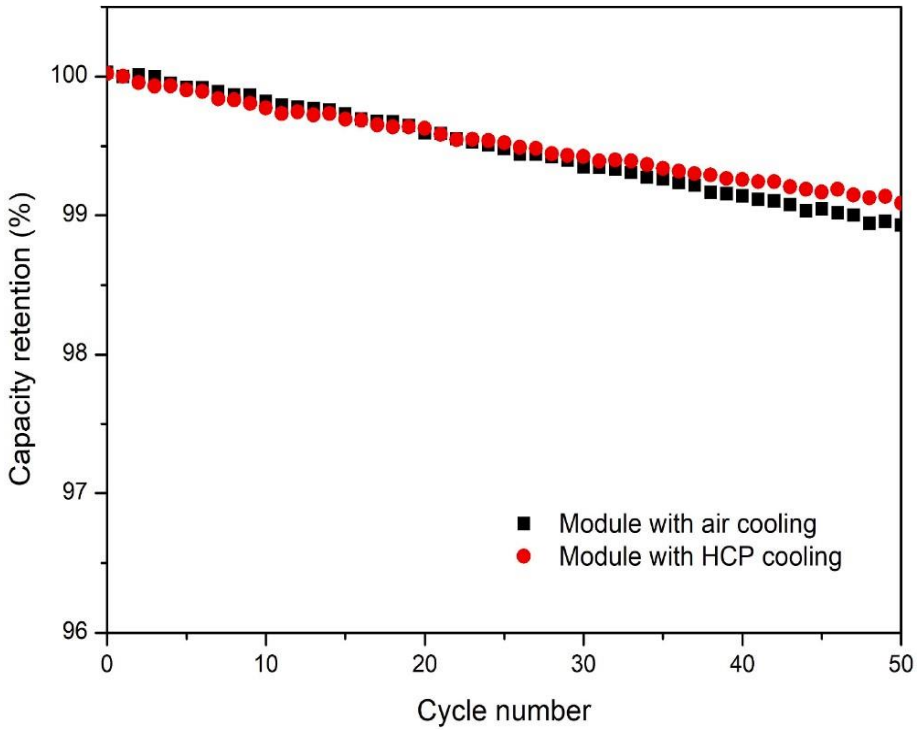

Air cooling P =

. 16. Capacity retention of the AC module and the HCP module during 50 cycles (1C/1C).

and uniform temperature distribution. From the point of view of energy consumption, air cooling was working for the module throughout an entire cycle, while the active cooling of HCP module was only performed during the constant voltage charging step and two pause steps, taking up 40% of the full cycle time. Therefore, HCP may be superior to the AC strategy in terms of temperature control and energy saving, and it is beneficial to maintaining battery capacity and prolong lifetime, as dis- cussed in the previous paragraph.

Thermal insulation effect

Simulation results show that HCP has thermal insulation effect under cold conditions [28]. Due to the energy storage characteristics of PCM, the heat absorbed from the batteries during charging and/or discharging can keep the temperature of batteries around the phase change tem- perature of the PCM during non-working period until its latent heat is completely released. To demonstrate the insulation effect of the HCP, the temperature changes of the battery pack and the battery module during the rest period without water cooling was investigated. The tests were conducted at 18˚C (air conditioner) and 10˚C (climate chamber) for pack and module, respectively. Due to the lack of a large refrigerated room, the pack has not been tested at a very low temperature.

As shown in Fig. 18(a), it is observed that the Tmin of the battery pack is maintained at 27˚C for ca. 170 min, which is the lower threshold of the melting temperature of PCM. However, the Tmax curve did not show an obvious plateau period. This is because the majority of the released heat was absorbed by the colder batteries instead of warmer ones, resulting in only 2˚C of ΔT after the phase change was completed. It is believed that

Section A-Research paper
ISSN 2063-5346

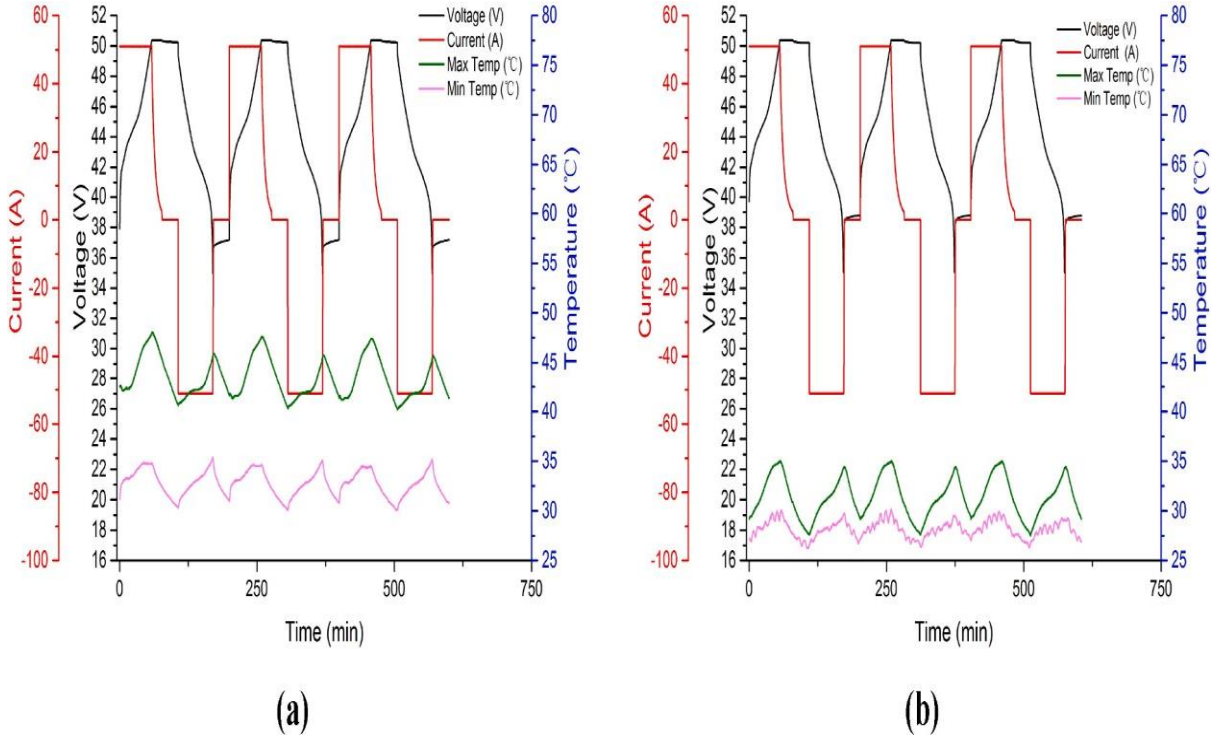

Fig. 17. Cycling performance of (a) the AC module and (b) the HCP module.

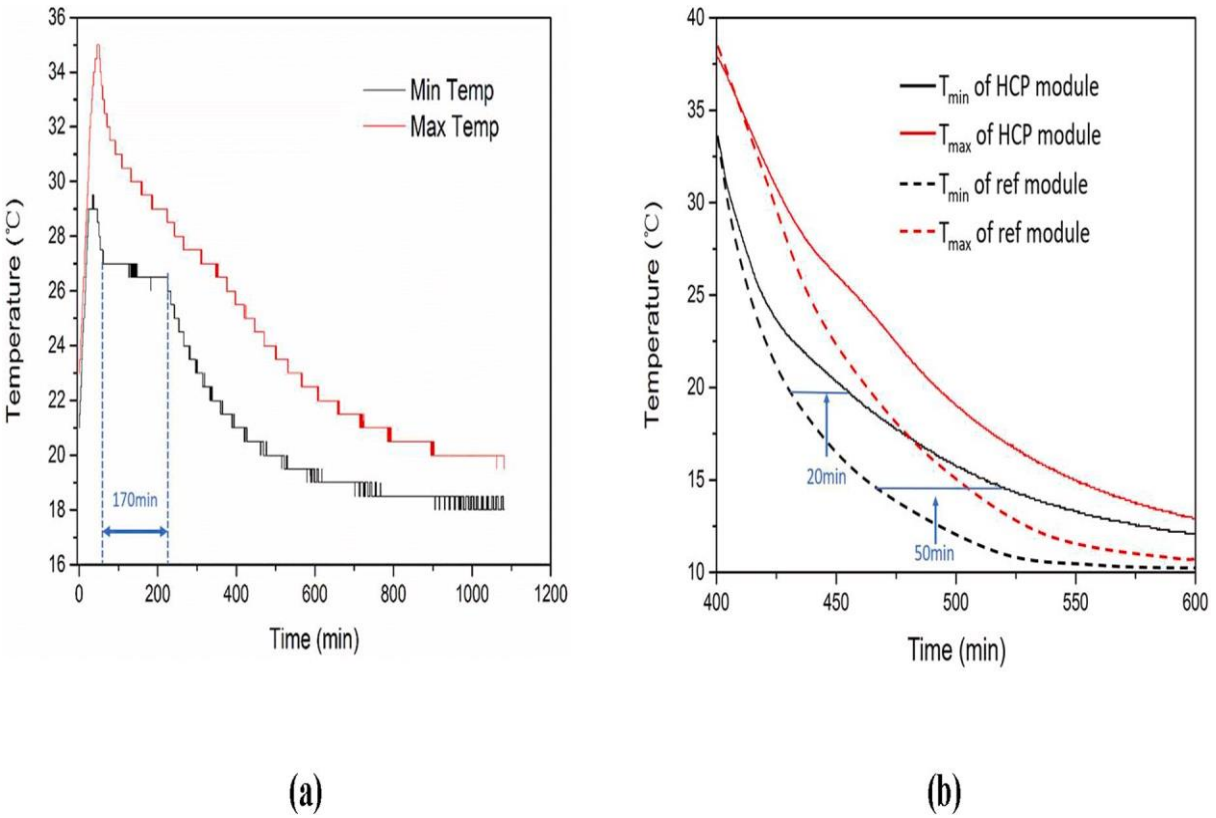

Fig. 18. Temperature decrease of (a) the battery pack at 18˚C and (b) the module at 10˚C.

the thermal insulation effect is still effective at a lower temperature, but the maintenance time is shorter. To demonstrate the speculation, the smaller HCP module was tested in a 10˚C climate chamber. As shown in Fig. 18(b), Tmax and Tmin decrease till the ambient temperature after almost 3 h. A slight convex on the curve appears from 27˚C to 22˚C for about 50 min. In contrast, the time for the reference module without insulation to decrease to 20˚C and 15˚C was advanced by 20 min and 50 min, respectively.

Remarks

A flaw of the general control strategy for 0.5C discharge scenario was found after initial trials. The problem was that, during dis- charging and pause phases, ΔT was<4.5˚C and the Tmax was about 28˚C, so active cooling was not required. Yet the constraints were satisfied, heat accumulation in the absence of water cooling considerably affected the following charging and caused 9˚C of ΔT. In order to meet the thermal management goal, active cooling was enforced during the pause step for restricting the Tmax below 24˚C. It suggests that on the mode of low power driving, active cooling is not requisite for the battery pack, but is essential during charging process to avoid overheating.

For the 1.5C discharge scenario, a large amount of heat enforced the cooling system to work at full capacity. Possible amendments for the control strategy are to apply lower TH or change the coolant flowing directions. The former is viable but the contri- bution of PCM becomes redundant; the latter requires additional mechanical work on pipeline system but is promising in improving temperature uniformity. In current design, the “hot zone” of the pack locates at the region of water outlet while the relative “colder zone” is located near the inlet. It shows an almost linear rise in temperature along the flow direction, which inspired that counter-current flow configurations for adjacent HCPs may make the temperature distribution of the battery pack more evenly.

Moreover, different from the side cooling design, the common- place solution from major pack manufacturers is bottom-cooling which is not only process sustainable, but also mechanically stable. Though a certain degree of heat exchange area is sacri- ficed, by taking advantage of the battery weight, the entire pack system has a high integration to better endure vibration and crash. Referring back to BMW i3 (2017 version) which also de- ploys a bottom liquid cooling plate and organic refrigerant for its battery pack, published data show that the operating temperature can be guaranteed ideally in the range of 25˚C to 40˚C [30,31]. Since the measurement is based on the standard dynamic driving profile in urban area at ambient temperature, it is hard to make solid comparison with our developed hybrid TMS. However, the test results in this paper show that PCMs do play a tangible role in energy-saving cooling and thermal insulation.

Conclusions

This paper presents the development of a prototype of a high- voltage battery pack for EVs with its hybrid thermal manage- ment system, an innovative hybrid cooling plate (HCP). The design of HCP focuses on the integration of active cooling with PCM. Firstly, no direct contact exists between batteries and PCM so the potential risk of liquid leakage could be avoided. Secondly, HCPs are easy to be installed or filled with different types of PCMs

thanks to the modular concept. Thirdly, the mechanical design of applying mandrel can efficiently enhance the latitudinal compression at pack level.

By customizing the specific control strategies, the cooling per- formance of HCPs for the pack under different discharge condi- tions is demonstrated. The operating temperature of the battery pack was controlled below 35˚C and the temperature difference was confined within 8˚C at discharge rates of 0.5C and 1C. For the high current 1.5C case, further technical improvements are required for reducing the maximum temperature which is now 40˚C. Meanwhile, the thermal insulation effect was verified as well. A significant delay for 170 min of temperature decreasing at phase change range was detected. Moreover, tests at module level also provided evidence for less capacity decay and more uniform temperature distribution from HCP in comparison with air cooling.

Under mild conditions, both in cooling and thermal insulation, PCM is sufficient to enhance temperature uniformity. Under extreme conditions, two specific scenarios should be considered. When batteries work in hot temperatures or at large currents, the role of PCM in cooling is not dominating due to the rapid release of a large amount of heat, and it is difficult to realize prompt heat exchange between materials and water or air. The thermophys- ical properties of PCMs suitable for TMS applications are difficult to be considerably improved in a short time. In this regard, active cooling is indispensable for the efficient cooling of the battery pack. If required, novel heat transfer fluids possessing higher heat carrying capacity can be used instead of water. When batteries start to run in extremely cold conditions, PCM solidates after releasing completely the latent heat so the insulation effect cannot perform. In this situation, active warming by circulating refrigerant or using PTC is necessary.

References

[1] Kennedy D, Philbin SP. Techno-economic analysis of the adoption of electric vehicles. Frontiers of Engineering Management. 2019;6:538–50.

[2] García-Olivares A, Sol´e J, Osychenko O. Transportation in a 100% renewable energy system. Energy Convers Manage 2018;158:266–85.

[3] Ding Y, Cano ZP, Yu A, Lu J, Chen Z. Automotive Li-Ion Batteries: Current Status and Future Perspectives. Electrochemical Energy Reviews. 2019;2(1):1–28.

[4] Duan J, Tang X, Dai H, Yang Y, Wu W, Wei X, et al. Building Safe Lithium-Ion Batteries for Electric Vehicles: A Review. Electrochemical Energy Reviews. 2020;3 (1):1–42.

[5]Kwade A, Haselrieder W, Leithoff R, Modlinger A, Dietrich F, Droeder K. Current status and challenges for automotive battery production technologies. Nat Energy 2018;3:290–300.

[6]Ma S, Jiang M, Tao P, Song C, Wu J, Wang J, et al. Temperature effect and thermal impact in lithium-ion batteries: A review. Progress in Natural Science: Materials International. 2018;28(6):653–66.

[7]Warner J. 7 - Lithium-Ion Battery Packs for EVs. In: Pistoia G, editor. Lithium-Ion Batteries. Amsterdam: Elsevier; 2014. p. 127–50.

[8]Liu H, Wei Z, He W, Zhao J. Thermal issues about Li-ion batteries and recent progress in battery thermal management systems: A review. Energy Convers Manage 2017;150:304–30.

[9)Zhao C, Zhang B, Zheng Y, Huang S, Yan T, Liu X. Hybrid Battery Thermal Management System in Electrical Vehicles: A Review. Energies. 2020;13(23):6257. https://doi.org/10.3390/en13236257.
[10]Saw LH, Tay AAO, Zhang LW. Thermal management of lithium-ion battery pack with liquid cooling. In: 2015 31st Thermal Measurement, Modeling & Management Symposium; (SEMI-THERM)2015.. p. 298–302.
[11]Lai Y, Wu W, Chen K, Wang S, Xin C. A compact and lightweight liquid-cooled thermal management solution for cylindrical lithium-ion power battery pack. Int J Heat Mass Transf 2019;144:118581.
[12]Wu W, Wang S, Wu W, Chen K, Hong S, Lai Y. A critical review of battery thermal performance and liquid based battery thermal management. Energy Convers Manage 2019;182:262–81.
[13]Hu X, Zheng Y, Howey DA, Perez H, Foley A, Pecht M. Battery warm-up methodologies at subzero temperatures for automotive applications: Recent advances and perspectives. Prog Energy Combust Sci 2020;77:100806. https://doi. org/10.1016/j.pecs.2019.100806.
[14]Ling Z, Zhang Z, Shi G, Fang X, Wang L, Gao X, et al. Review on thermal management systems using phase change materials for electronic components, Li- ion batteries and photovoltaic modules. Renew Sustain Energy Rev 2014;31: 427–38.
[15]Lyu Y, Siddique ARM, Majid SH, Biglarbegian M, Gadsden SA, Mahmud S. Electric vehicle battery thermal management system with thermoelectric cooling. Energy Rep 2019;5:822–7.
[16]Mei N, Xu X, Li R. Heat Dissipation Analysis on the Liquid Cooling System Coupled with a Flat Heat Pipe of a Lithium-Ion Battery. ACS Omega 2020;5:17431–41.
[17]Hallaj SA, Selman JR. A Novel Thermal Management System for Electric Vehicle Batteries Using Phase-Change Material. J Electrochem Soc 2000;147:3231.
[18]Al-Hallaj S, Selman JR. Thermal modeling of secondary lithium batteries for electric vehicle/hybrid electric vehicle applications. J Power Sources 2002;110: 341–8.
[19]Verma A, Shashidhara S, Rakshit D. A comparative study on battery thermal management using phase change material (PCM). Thermal Science and Engineering Progress. 2019;11:74–83.
[20]Wang X, Xie Y, Day R, Wu H, Hu Z, Zhu J, et al. Performance analysis of a novel thermal management system with composite phase change material for a lithium- ion battery pack. Energy. 2018;156:154–68.
[21]Abujas CR, Jove´ A, Prieto C, Gallas M, Cabeza LF. Performance comparison of a group of thermal conductivity enhancement methodology in phase change material for thermal storage application. Renewable Energy 2016;97:434–43.
[22]Barnes D, Li X. Battery Thermal Management Using Phase Change Material-Metal Foam Composite Materials at Various Environmental Temperatures. J Electrochem Energy Convers Storage 2019;17.
[23]Zheng N, Fan R, Sun Z, Zhou T. Thermal management performance of a fin- enhanced phase change material system for the lithium-ion battery. Energy Res. 2020;44:7617–29.

[24]Barsotti DL, Hyatt WT, Compere MD, Boetcher SKS. Battery Thermal Management for Hybrid Electric Vehicles Using a Phase-Change Material Cold Plate. ASME 2013 Heat
[25]Transfer Summer Conference collocated with the ASME 2013 7th International
[26]Conference on Energy Sustainability and the ASME 2013 11th International Conference on Fuel Cell Science, Engineering and Technology. 2013.
[27]Bai F, Chen M, Song W, Feng Z, Li Y, Ding Y. Thermal management performances of PCM/water cooling-plate using for lithium-ion battery module based on non- uniform internal heat source. Appl Therm Eng 2017;126:17–27.
[28]Kiani M, Ansari M, Arshadi AA, Houshfar E, Ashjaee M. Hybrid thermal management of lithium-ion batteries using nanofluid, metal foam, and phase change material: an integrated numerical–experimental approach. J Therm Anal Calorim 2020;141:1703–15.
[29]Yu GY, Chiang SW, Chen W, Du HD. Thermal Management of a Li-Ion Battery for Electric Vehicles Using PCM and Water-Cooling Board. Key Eng Mater 2019;814: 307–13.
[30]Akbarzadeh M, Jaguemont J, Kalogiannis T, Karimi D, He J, Jin L, et al. A novel liquid cooling plate concept for thermal management of lithium-ion batteries in electric vehicles. Energy Convers Manage 2021;231:113862.
[31]Li Z, Zhang J, Wu B, Huang J, Nie Z, Sun Y, et al. Examining temporal and spatial variations of internal temperature in large-format laminated battery with embedded thermocouples. J Power Sources 2013;241:536–53.
[33)F. Schoewel; E.Hochgeiger, The high voltage batteries of the BMW i3 and BMW i8. In Proceedings of the Advanced Automotive Battery Conference, Atlanta, GA, USA, 3 February 2014.
https://www.youtube.com/watch?v=PG3kYPxR_ak.